



**HAL**  
open science

## 6-Chloro-3-nitro-2-[(phenylsulfonyl)methyl]imidazo[1,2-b]pyridazine

Romain Paoli-Lombardo, Nicolas Primas, Sébastien Hutter, Sandra Bourgeade-Delmas, Clotilde Boudot, Caroline Castera-Ducros, Inès Jacquet, Bertrand Courtioux, Nadine Azas, Pascal Rathelot, et al.

► **To cite this version:**

Romain Paoli-Lombardo, Nicolas Primas, Sébastien Hutter, Sandra Bourgeade-Delmas, Clotilde Boudot, et al.. 6-Chloro-3-nitro-2-[(phenylsulfonyl)methyl]imidazo[1,2-b]pyridazine. Molbank, 2023, Molbank, 2023 (1), pp.M1573. 10.3390/m1573. hal-04115477

**HAL Id: hal-04115477**

**<https://amu.hal.science/hal-04115477>**

Submitted on 17 Jul 2023

**HAL** is a multi-disciplinary open access archive for the deposit and dissemination of scientific research documents, whether they are published or not. The documents may come from teaching and research institutions in France or abroad, or from public or private research centers.





L'archive ouverte pluridisciplinaire **HAL**, est destinée au dépôt et à la diffusion de documents scientifiques de niveau recherche, publiés ou non, émanant des établissements d'enseignement et de recherche français ou étrangers, des laboratoires publics ou privés.



Distributed under a Creative Commons Attribution 4.0 International License

Short Note

# 6-Chloro-3-nitro-2-[(phenylsulfonyl)methyl]imidazo[1,2-*b*]pyridazine

Romain Paoli-Lombardo <sup>1</sup>, Nicolas Primas <sup>1,2,\*</sup> , Sébastien Hutter <sup>3</sup>, Sandra Bourgeade-Delmas <sup>4</sup>, Clotilde Boudot <sup>5</sup>, Caroline Castera-Ducros <sup>1,2</sup>, Inès Jacquet <sup>1</sup>, Bertrand Courtioux <sup>5</sup> , Nadine Azas <sup>3</sup>, Pascal Rathelot <sup>1,2</sup>  and Patrice Vanelle <sup>1,2,\*</sup> 

<sup>1</sup> CNRS, ICR UMR 7273, Team Pharmaco-Chimie Radicalaire, Faculty of Pharmacy, Aix Marseille University, 27 Boulevard Jean Moulin, CS30064, CEDEX 05, 13385 Marseille, France

<sup>2</sup> Central Service for Pharmaceutical Quality and Information SCQIP, Pharmacy Department, Hospital Conception, AP-HM, 13005 Marseille, France

<sup>3</sup> IHU Méditerranée Infection, UMR VITROME—Tropical Eukaryotic Pathogens, Aix Marseille University, 19–21 Boulevard Jean Moulin, 13005 Marseille, France

<sup>4</sup> UMR 152 PHARMA-DEV, University of Toulouse, IRD, UPS, 31062 Toulouse, France

<sup>5</sup> Faculty of Pharmacy, Institute of Neuroepidemiology and Tropical Neurology, University of Limoges, INSERM U1094, 87025 Limoges, France

\* Correspondence: nicolas.primas@univ-amu.fr (N.P.); patrice.vanelle@univ-amu.fr (P.V.)

**Abstract:** As part of our ongoing scaffold-hopping work on an antikinoplastid 3-nitroimidazo[1,2-*a*]pyridine scaffold, we explored 3-nitroimidazo[1,2-*b*]pyridazine as a potential new antikinoplastid series. Using conditions previously described by our lab, we obtained 6-chloro-3-nitro-2-[(phenylsulfonyl)methyl]imidazo[1,2-*b*]pyridazine with 54% yield. In vitro activity of this compound was evaluated against both the promastigote form of *Leishmania donovani*, the axenic amastigote form of *Leishmania infantum* and the trypomastigote blood stream form of *Trypanosoma brucei*, and its influence on cell viability was assessed on the HepG2 cell line. However, despite good activity against the trypomastigote blood stream form of *T. b. brucei* (EC<sub>50</sub> = 0.38 μM), it showed poor solubility in both HepG2 (CC<sub>50</sub> > 7.8 μM) and *L. infantum* axenic amastigotes (EC<sub>50</sub> > 1.6 μM) culture media, associated with a loss of activity against the promastigote form of *L. infantum* (EC<sub>50</sub> > 15.6 μM).

**Keywords:** imidazo[1,2-*b*]pyridazine; nitroaromatic; scaffold-hopping; structure-activity relationships; *Leishmania* spp.; *Trypanosoma brucei*



**Citation:** Paoli-Lombardo, R.; Primas, N.; Hutter, S.; Bourgeade-Delmas, S.; Boudot, C.; Castera-Ducros, C.; Jacquet, I.; Courtioux, B.; Azas, N.; Rathelot, P.; et al. 6-Chloro-3-nitro-2-[(phenylsulfonyl)methyl]imidazo[1,2-*b*]pyridazine. *Molbank* **2023**, *2023*, M1573. <https://doi.org/10.3390/M1573>

Academic Editor: Fawaz Aldabbagh

Received: 17 January 2023

Revised: 28 January 2023

Accepted: 30 January 2023

Published: 1 February 2023



**Copyright:** © 2023 by the authors. Licensee MDPI, Basel, Switzerland. This article is an open access article distributed under the terms and conditions of the Creative Commons Attribution (CC BY) license (<https://creativecommons.org/licenses/by/4.0/>).

## 1. Introduction

Kinetoplastids are a group of flagellated protozoa responsible for neglected tropical diseases (NTDs) in mammals, including leishmaniasis (*Leishmania* spp.) and sleeping sickness (*Trypanosoma brucei*) [1]. These two diseases are found in developing countries, especially in tropical environments. More than 1 billion people are at risk of infection, and nearly 20 million people are infected, causing up to 50,000 deaths per year [2,3]. With an estimated 50,000–90,000 new cases each year, life-threatening visceral leishmaniasis (VL), caused by *Leishmania infantum* in the Mediterranean Basin and Latin America and *L. donovani* in Asia and Africa, is responsible for more than 30,000 deaths annually [4,5]. Sleeping sickness is endemic in 36 countries throughout sub-Saharan Africa and 60 million people are considered to be at risk of contracting this disease [6]. Unfortunately, in the absence of a vaccine [7], treatment of VL and sleeping sickness is based on a small number of drugs, most of them associated with significant toxicity, increasing resistance, and constraining administration [8].

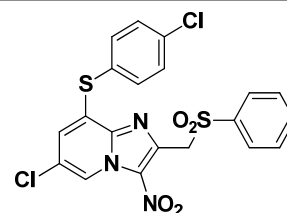
The main distinguishing feature of the kinetoplastids is a subcellular structure known as a kinetoplast. Several different morphological forms of kinetoplasts have been observed and are associated with different life cycle stages in various species. *Leishmania* parasites

have two main life cycle stages: the promastigote form (found in the insect vector) and the amastigote form (inside the mammalian host). Because promastigotes are easier to obtain and maintain, they are only a preliminary evaluation for drug screening with the risk of identifying compounds that are potentially ineffective in humans. Intramacrophagic amastigotes are therefore the best model for drug evaluation but are more difficult to obtain. An alternative is to use axenic amastigotes, adapted to grow outside their host cell (macrophages) in a growth medium that mimics intracellular conditions. Trypanosomatids also have several different classes of cellular organization, two of which are adopted by *T. brucei* at different stages of the life cycle: epimastigotes are found in the tsetse fly vector, while trypomastigotes are found in mammalian hosts, primarily in the blood, and are referred as bloodstream forms (BSF).

With the aim of developing new antikinoplastid molecules, our team previously identified a hit compound in 3-nitroimidazo[1,2-*a*]pyridine series (Hit A), bearing a phenylsulfonmethyl substituent at position 2, a chlorine at position 6 and a 4-chlorophenylthioether moiety at position 8 (Table 1) [9]. This compound displayed low cytotoxicity (cytotoxic concentration 50% = CC<sub>50</sub>) on human hepatocyte HepG2 cell line, associated with micromolar in vitro activities (measured through effective concentration 50% = EC<sub>50</sub>) against both the promastigote form of *L. donovani*, the axenic amastigote form of *L. infantum* and the trypomastigote blood stream form (BSF) of *T. b. brucei*.

**Table 1.** Structure and biological profile of previously identified Hit A.

	Hit A
EC <sub>50</sub> <i>L. donovani</i> promastigotes (μM)	1.0 ± 0.3
EC <sub>50</sub> <i>L. infantum</i> axenic amastigotes (μM)	1.7 ± 0.3
EC <sub>50</sub> <i>T. b. brucei</i> BSF (μM)	0.95 ± 0.05
CC <sub>50</sub> HepG2 (μM)	>100



As part of our ongoing medicinal chemistry work to improve Hit A properties, a scaffold-hopping strategy on the 3-nitroimidazo[1,2-*a*]pyridine core was implemented for structure–activity relationship purposes. This scaffold-hopping approach allowed the discovery of structurally new compounds, from known active molecules, by modification of their core [10]. By replacing the carbon atom at position 5 of the 3-nitroimidazo[1,2-*a*]pyridine moiety with a nitrogen atom, a new 3-nitroimidazo[1,2-*b*]pyridazine moiety was obtained (Figure 1).

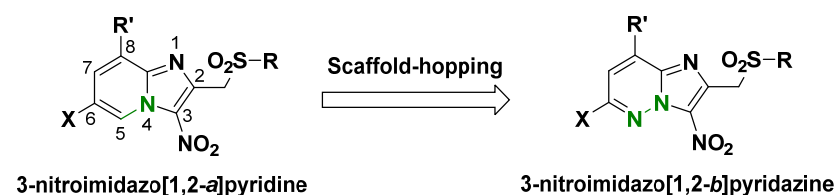
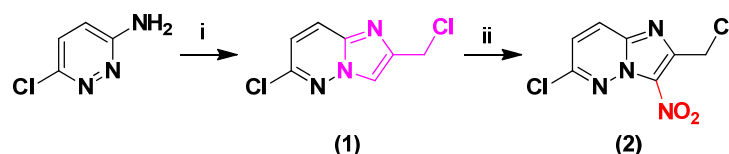


**Figure 1.** Scaffold-hopping strategy of 3-nitroimidazo[1,2-*a*]pyridine moiety into 3-nitroimidazo[1,2-*b*]pyridazine moiety.

## 2. Results and Discussion

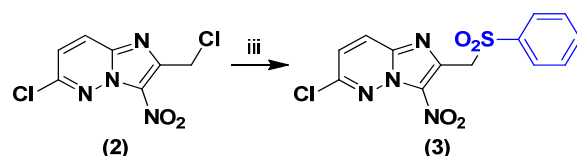
### 2.1. Synthesis

Adapting a previously reported synthetic route developed in our lab [11], intermediate **1** was obtained by the cyclocondensation of 1,3-dichloroacetone with commercially available 3-amino-6-chloropyridazine in refluxing 1,2-dimethoxyethane, followed by a nitration reaction at position 3, giving the 2-chloromethyl-3-nitroimidazo[1,2-*b*]pyridazine **2** (Scheme 1).



**Scheme 1.** Synthesis of compounds **1** and **2**. Reagents and conditions: (i) 1,3-Dichloroacetone 1.1 equiv, DME, 90 °C, 37%; (ii) HNO<sub>3</sub> 68% 6 equiv, H<sub>2</sub>SO<sub>4</sub>, 0 °C → RT, 98%.

Finally, compound **3** was prepared in moderate yield by substituting the chlorine atom of the chloromethyl group at position 2 of substrate **2** with sodium benzenesulfinate (Scheme 2).



**Scheme 2.** Synthesis of compound **3**. Reagents and conditions: (iii) Sodium benzenesulfinate 3 equiv, DMSO, RT, 15 h, 54%.

### 2.2. Biological Results

In order to compare its biological profile to Hit **A** and to reference drugs (amphotericin B, miltefosine, fexinidazole and suramin), the activity of compound **3** was evaluated in vitro against the promastigote form of *L. donovani*, the axenic amastigote form of *L. infantum* and the trypomastigote blood stream form of *T. b. brucei*. Its influence on cell viability was assessed on the HepG2 cell line, using doxorubicin as a positive control (Table 2).

**Table 2.** In vitro evaluation of molecule **3** on *L. donovani* promastigotes, *L. infantum* axenic amastigotes, *T. b. brucei* trypomastigotes (BSF) and the human hepatocyte HepG2 line.

	CC <sub>50</sub> HepG2 (μM)	EC <sub>50</sub> <i>L. dono.</i> pro. (μM)	EC <sub>50</sub> <i>L. inf.</i> Axenic Ama. (μM)	EC <sub>50</sub> <i>T. b. brucei</i> BSF (μM)
<b>3</b>	>7.8 <sup>a</sup>	>15.6 <sup>a</sup>	>1.6 <sup>a</sup>	0.38 ± 0.03
Hit A	>100	1.0 ± 0.3	1.7 ± 0.3	0.95 ± 0.05
Doxorubicin <sup>b</sup>	0.20 ± 0.02	-	-	-
Amphotericin B <sup>c</sup>	8.8 ± 0.3	0.07 ± 0.01	0.08 ± 0.02	-
Miltefosine <sup>c</sup>	85.0 ± 8.8	3.1 ± 0.2	0.30 ± 0.02	-
Fexinidazole <sup>c,d</sup>	>100	1.2 ± 0.2	7.8 ± 2.3	1.4 ± 0.5
Suramin <sup>d</sup>	>100	-	-	0.08 ± 0.04

<sup>a</sup> The product could not be tested at higher concentrations due to a lack solubility in the culture medium.

<sup>b</sup> Doxorubicin was used as a cytotoxic reference drug. <sup>c</sup> Amphotericin B, Miltefosine, and Fexinidazole were used as antileishmanial reference drugs. <sup>d</sup> Fexinidazole and Suramin were used as anti-*Trypanosoma brucei* reference drugs.

Compound **3** displayed submicromolar in vitro activities against the trypomastigote blood stream form of *T. b. brucei* (EC<sub>50</sub> = 0.38 μM), better than Hit **A** (EC<sub>50</sub> = 0.95 μM) and the reference drug fexinidazole (EC<sub>50</sub> = 1.4 μM). However, it showed poor solubility in both HepG2 (CC<sub>50</sub> > 7.8 μM) and *L. infantum* axenic amastigotes (EC<sub>50</sub> > 1.6 μM) culture media, associated with a loss of activity against the promastigote form of *L. infantum* (EC<sub>50</sub> > 15.6 μM).

Thus, because of the lack of solubility and the loss of antileishmanial activity of compound **3**, the continuation of the scaffold-hopping work on the 3-nitroimidazo[1,2-*b*]pyridazine series has been suspended for the moment.

### 3. Materials and Methods

#### 3.1. Chemistry

##### 3.1.1. General

Melting points were determined on a Köfler melting point apparatus (Wagner & Munz GmbH, München, Germany) and were uncorrected. Elemental analyses were carried out at the Spectropole, Faculté des Sciences de Saint-Jérôme (Marseille) with a Thermo Finnigan EA1112 analyzer (Thermo Finnigan, San Jose, CA, USA). NMR spectra were recorded on a Bruker Avance 250MHz or a Bruker Avance NEO 400MHz NanoBay spectrometer at the Faculté de Pharmacie of Marseille. (<sup>1</sup>H NMR: reference CDCl<sub>3</sub> δ = 7.26 ppm, reference DMSO-*d*<sub>6</sub> δ = 2.50 ppm and <sup>13</sup>C NMR: reference CDCl<sub>3</sub> δ = 76.9 ppm, reference DMSO-*d*<sub>6</sub> δ = 39.52 ppm.) The following adsorbent was used for column chromatography: silica gel 60 (Merck KGaA, Darmstadt, Germany, particle size 0.063–0.200 mm, 70–230 mesh ASTM). TLC was performed on 5 cm × 10 cm aluminum plates coated with silica gel 60F-254 (Merck) in an appropriate eluent. Visualization was performed with ultraviolet light (254 nm). Purity determination of synthesized compounds was checked by LC/MS analyses, which were realized at the Faculté de Pharmacie of Marseille with a Thermo Scientific Accela High Speed LC System<sup>®</sup> (Waltham, MA, USA) coupled using a single quadrupole mass spectrometer Thermo MSQ Plus<sup>®</sup>. The purity of the synthesized compound **3** was >95%. The RP-HPLC column was a Thermo Hypersil Gold<sup>®</sup> 50 × 2.1 mm (C<sub>18</sub> bounded), with particles of a diameter of 1.9 μm. The volume of sample injected on the column was 1 μL. Chromatographic analysis, for a total duration of 8 min, was on the gradient of the following solvents: t = 0 min, methanol/water 50:50; 0 < t < 4 min, linear increase in the proportion of methanol to a methanol/water ratio of 95:5; 4 < t < 6 min, methanol/water 95:5; 6 < t < 7 min, linear decrease in the proportion of methanol to return to a methanol/water ratio of 50:50; 6 < t < 7 min, methanol/water 50:50. The water used was buffered with ammonium acetate 5 mM. The flow rate of the mobile phase was 0.3 mL/min. The retention times (t<sub>R</sub>) of the molecules analyzed were indicated in min. Reagents were purchased from Sigma-Aldrich or Fluorochem and used without further purification. Copies of <sup>1</sup>H and <sup>13</sup>C NMR spectra are available in the Supplementary Materials.

##### 3.1.2. 6-Chloro-2-(chloromethyl)imidazo[1,2-*b*]pyridazine (**1**)

To a solution of 6-chloropyridazin-3-amine (5 g, 38.60 mmol, 1 equiv) in 1,2-dimethoxyethane (80 mL), 1,3-dichloroacetone (4.90 g, 38.60 mmol, 1.1 equiv) was added. The reaction mixture was stirred and heated under reflux for 48 h. Then, the solvent was evaporated in vacuo. Compound **1** was obtained after purification by chromatography on silica gel (eluent: dichloromethane-ethyl acetate 9:1) as a white solid in 37% yield (2.9 g). mp 154 °C. <sup>1</sup>H NMR (250 MHz, CDCl<sub>3</sub>) δ: 7.96 (s, 1H), 7.87 (d, *J* = 9.5 Hz, 1H), 7.09 (d, *J* = 9.5 Hz, 1H), 4.76 (s, 1H). <sup>13</sup>C NMR (63 MHz, CDCl<sub>3</sub>) δ: 146.1, 144.7, 136.9, 125.3, 118.3, 115.1, and 36.5.

##### 3.1.3. 6-Chloro-2-(chloromethyl)-3-nitroimidazo[1,2-*b*]pyridazine (**2**)

To a solution of 6-chloro-2-(chloromethyl)imidazo[1,2-*b*]pyridazine (**1**) (2 g, 9.90 mmol, 1 equiv) in concentrated sulfuric acid (20 mL) cooled by an ice-water bath, nitric acid 68% (2.6 mL, 59.40 mmol, 6 equiv) was added dropwise. The reaction mixture was stirred for 3 h at room temperature. Then, the mixture was slowly poured into an ice-water mixture and precipitated. The solid was collected by filtration and dried under reduced pressure. Compound **2** was obtained without further purification as a white solid in 98% yield (2.4 g). mp 196 °C. <sup>1</sup>H NMR (250 MHz, CDCl<sub>3</sub>) δ: 8.10 (d, *J* = 9.6 Hz, 1H), 7.48 (d, *J* = 9.5 Hz, 1H), 5.11 (s, 2H). <sup>13</sup>C NMR (63 MHz, CDCl<sub>3</sub>) δ: 150.3, 145.1, 137.3, 127.8, 124.5, and 38.3.

### 3.1.4. 6-Chloro-3-nitro-2-[(phenylsulfonyl)methyl]imidazo[1,2-*b*]pyridazine (3)

To a solution of 6-chloro-2-(chloromethyl)-3-nitroimidazo[1,2-*b*]pyridazine (2) (0.5 g, 2.02 mmol, 1 equiv) in dimethylsulfoxide (40 mL), sodium benzenesulfinate (0.99 g, 6.06 mmol, 3 equiv) was added. The reaction mixture was stirred for 15 h at room temperature. Then, the mixture was slowly poured into an ice-water mixture and precipitated. The solid was collected by filtration and dried under reduced pressure. Compound 3 was obtained after purification by chromatography on silica gel (eluent: dichloromethane-ethyl acetate 9:1) as a white solid in 54% yield (0.385 g). mp 253 °C. <sup>1</sup>H NMR (400 MHz, DMSO-*d*<sub>6</sub>) δ: 8.48 (d, *J* = 9.6 Hz, 1H), 7.88 (d, *J* = 9.6 Hz, 1H), 7.79–7.70 (m, 3H), 7.64–7.56 (m, 2H), and 5.23 (s, 2H). <sup>13</sup>C NMR (100 MHz, DMSO-*d*<sub>6</sub>) δ: 149.4, 138.5, 138.0, 137.1, 134.3, 132.3, 129.4 (2C), 128.8, 128.0 (2C), 125.4, and 55.9. LC/MS ESI+ *t*<sub>R</sub> 0.90, (*m/z*) [M+H]<sup>+</sup> 353.13/355.10. HRMS (+ESI): 353.0105 [M+H]<sup>+</sup>. Calcd for C<sub>13</sub>H<sub>10</sub>ClN<sub>4</sub>O<sub>4</sub>S: 353.0106.

## 3.2. Biology

### 3.2.1. Antileishmanial Activity against *L. donovani* Promastigotes

The *Leishmania* species used in this study was *L. donovani* (MHOM/IN/00/DEVI) purchased from CNR Leishmania (Montpellier, France). *Leishmania* promastigote forms were grown in Schneider's Drosophila medium (Life Technologies, Saint-Aubin, France) supplemented with 100 U/mL penicillin, 100 µg/mL streptomycin, 2 mM L-glutamine and 20% FCS (Life Technologies, Saint-Aubin, France) at 27 °C. The in vitro evaluation of the tested compound's antileishmanial activity on promastigote forms was carried out by MTT assay according to the Mosmann protocol [12] with some modifications. Briefly, promastigotes in log-phase were incubated at an average density of 10<sup>6</sup> parasites/mL in sterile 96-well plates with various concentrations of compound dissolved in DMSO (final concentration less than 0.5% *v/v*), in duplicate. Appropriate controls treated with DMSO, Miltefosine, Amphotericin B and Fexinidazole (reference drugs purchased from Sigma-Aldrich, Saint-Louis, MI, USA) were added to each set of experiments. After a 72h incubation period at 27 °C, parasitic metabolic activity was determined. Each plate-well was then microscope-analyzed to detect any precipitate formation. A total of 20 µL of MTT (3-(4,5-dimethylthiazol-2-yl)-2,5-diphenyltetrazolium bromide) (Sigma-Aldrich, Saint-Louis, MI, USA) solution (5 mg/mL in PBS) was added to each well and incubated for 4 h at 27 °C. The enzyme reaction was then stopped by addition of 100 µL of 50% isopropanol–10% sodium dodecyl sulfate. Plates were shaken vigorously at 300 rpm for 10 min. The absorbance was measured at 570 nm in a BIO-TEK Elx808 (Biotek, Colmar, France) absorbance microplate reader. An inhibitory concentration of 50% (EC<sub>50</sub>) was defined as the concentration of drug required to inhibit the metabolic activity of *Leishmanial* promastigote forms by 50% relative to the control. EC<sub>50</sub> values were calculated by non-linear regression analysis processed dose–response curves, using TableCurve 2D V5.0 software. EC<sub>50</sub> values represent the mean value calculated from at least three separate experiments.

### 3.2.2. Antileishmanial Activity on *L. infantum* Axenic Amastigotes

*L. infantum* promastigotes were harvested in the logarithmic phase of growth by centrifugation at 900 g for 10 min. The supernatant was removed carefully and was replaced by the same volume of RPMI 1640 complete medium at pH 5.4 and incubated for 24 h at 24 °C. The acidified promastigotes were then incubated for 24 h at 37 °C in a ventilated flask to transform them into axenic amastigotes. The amastigote stage was checked both by electron microscopy (short flagellum with small bulbous tip extending beyond a spherical cell body) and RT-PCR to confirm the overexpression of ATG8 and amastin genes in amastigotes, relative to promastigotes. The effects of the tested compounds on the growth of *L. infantum* axenic amastigotes were assessed as follows. *L. infantum* amastigotes were incubated at a density of 2 × 10<sup>6</sup> parasites/mL in sterile 96-well plates with various concentrations of a compound dissolved in DMSO (final concentration less than 0.5% *v/v*), in duplicate. Appropriate controls treated with DMSO, Amphotericin B, Miltefosine, and

Fexinidazole were added to each set of experiments. After a 48 h incubation period at 37 °C, each plate-well was then microscopically examined to detect any precipitate formation.

Luciferase activity and determination of EC<sub>50</sub> were performed as above.

### 3.2.3. Antitrypanosomal Evaluation on *T. b. brucei* BSF Trypomastigotes

The effects of the tested compounds on the growth of *T. b. brucei* were assessed by Alamar Blue<sup>®</sup> assay described by R  z et al. [13]. *T. b. brucei* AnTat 1.9 (IMTA, Antwerpen, Belgium) was cultured in MEM with Earle's salts, supplemented according to the protocol of Baltz et al. [14] with the following modifications: 0.5 mM mercaptoethanol (Sigma Aldrich<sup>®</sup>, Saint-Quentin-Fallavier, France), 1.5 mM L-cysteine (Sigma Aldrich<sup>®</sup>), 0.05 mM bathocuproine sulfate (Sigma Aldrich<sup>®</sup>) and 20% heat-inactivated horse serum (Gibco<sup>®</sup>, France), at 37 °C and 5% CO<sub>2</sub>. They were incubated at an average density of 2000 parasites/100 µL in sterile 96-well plates (Fisher<sup>®</sup>, France) with various concentrations of compound dissolved in DMSO, in duplicate. Appropriate controls suramin, treated with sterile water, and fexinidazole, treated with DMSO on sterile water (reference drugs purchased from Sigma Aldrich, France and Fluorochem, UK), were added to each set of experiments. After a 69 h incubation period at 37 °C, 10 µL of the viability marker Alamar Blue<sup>®</sup> (Fisher, France) was then added to each well, and the plates were incubated for 5 h. The plates were read in an ENSPIRE microplate reader (PerkinElmer) using an excitation wavelength of 530 nm and an emission wavelength of 590 nm. EC<sub>50</sub> was defined as the concentration of the drug necessary to inhibit the activity of *T. b. brucei* by 50% relative to the control. EC<sub>50</sub> values were calculated by nonlinear regression analysis processed on dose–response curves, using GraphPad Prism software (USA). EC<sub>50</sub> values were calculated from three separate experiments.

### 3.2.4. Cytotoxicity Evaluation on HepG2 Cell Line

HepG2 cell line (hepatocarcinoma cell line purchased from ATCC, ref HB-8065) was maintained at 37 °C, 5% CO<sub>2</sub> with 90% humidity in MEM supplemented with 10% fetal bovine serum, 1% L-glutamine (200 mM) and penicillin (100 U/mL)/streptomycin (100 mg/mL) (complete MEM medium). The tested molecules' cytotoxicity was assessed according to the method of Mosmann [12] with slight modifications. Briefly, 5 × 10<sup>3</sup> cells in 100 µL of complete medium were inoculated into each well of 96-well plates and incubated at 37 °C in a humidified 5% CO<sub>2</sub>. After 24 h incubation, 100 µL of medium with various product concentrations dissolved in DMSO (final concentration less than 0.5% v/v) were added, and the plates were incubated for 72 h at 37 °C. Triplicate assays were performed for each sample. Each plate-well was then microscope-examined to detect possible precipitate formation before the medium was aspirated from the wells. In total, 100 µL of MTT (3-(4,5-dimethyl-2-thiazolyl)-2,5-diphenyl-2H-tetrazolium bromide) solution (0.5 mg/mL in medium without FCS) was then added to each well. Cells were incubated for 2 h at 37 °C, following which the MTT solution was removed and DMSO (100 µL) was added to dissolve the resulting blue formazan crystals. Plates were shaken vigorously (700 rpm) for 10 min. The absorbance was measured at 570 nm with 630 nm as the reference wavelength using a BIO-TEK ELx808 Absorbance Microplate Reader. DMSO was used as blank and doxorubicin (purchased from Sigma Aldrich) as positive control. Cell viability was calculated as percentage of control (cells incubated without compound). The 50% cytotoxic concentration (CC<sub>50</sub>) was determined from the dose–response curve by using the TableCurve 2D v5.0 software (Jandel scientific). CC<sub>50</sub> values represent the mean value calculated from three separate experiments.

## 4. Conclusions

Based on a previously identified antikinoplastid Hit A in our lab, using a ring variation strategy, we reported the synthesis of 6-chloro-3-nitro-2-[(phenylsulfonyl)methyl]imidazo[1,2-*b*]pyridazine. Biological assessment showed that despite a good in vitro activity against the trypomastigote blood stream form of *T. b. brucei* (EC<sub>50</sub> = 0.38 µM), a poor

solubility in culture media impaired the determination of cytotoxicity (HepG2 CC<sub>50</sub> > 7.8 µM) and the activity against *L. infantum* axenic amastigotes (EC<sub>50</sub> > 1.6 µM) and the promastigote form of *L. infantum* (EC<sub>50</sub> > 15.6 µM).

In conclusion, future work on the 3-nitroimidazo[1,2-*b*]pyridazine series will require the introduction of more polar substituents to enhance the aqueous solubility of the derivatives.

**Supplementary Materials:** The following supporting information can be online. <sup>1</sup>H and <sup>13</sup>C NMR spectra.

**Author Contributions:** Conceptualization, N.P.; methodology, N.P., N.A. and B.C.; validation, N.P., N.A. and B.C.; formal analysis, R.P.-L., S.B.-D., S.H., C.B. and I.J.; investigation, R.P.-L., S.B.-D., S.H., C.B. and I.J.; resources, P.V., N.A. and B.C.; writing—original draft preparation, R.P.-L.; writing—review and editing, N.P., P.V., N.A., P.R. and C.C.-D.; supervision, N.P., P.V., P.R., P.V., N.A. and B.C.; project administration, N.P. and P.V. All authors have read and agreed to the published version of the manuscript.

**Funding:** This research was funded by “Aix-Marseille Université (AMU)”, by “Centre national de la recherche scientifique (CNRS)” and by “Assistance publique—Hôpitaux de Marseille (AP-HM)”.

**Data Availability Statement:** Not applicable.

**Acknowledgments:** We want to thank Vincent Remusat (Institut de Chimie Radicalaire, Marseille) for his help with NMR analysis, Valérie Monnier and Gaëlle Hisler (Spectropole, Marseille) for performing HRMS analysis.

**Conflicts of Interest:** The authors declare no conflict of interest. The funders had no role in the design of the study; in the collection, analyses, or interpretation of data; in the writing of the manuscript; or in the decision to publish the results.

## References

1. Ren, B.; Gupta, N. Taming Parasites by Tailoring Them. *Front. Cell. Infect. Microbiol.* **2017**, *7*, 292. [CrossRef] [PubMed]
2. Bruschi, F.; Gradoni, L. (Eds.) *The Leishmaniases: Old Neglected Tropical Diseases*; Springer International Publishing: Cham, Switzerland, 2018; ISBN 978-3-319-72385-3.
3. World Health Organization (WHO). Trypanosomiasis, Human African (Sleeping Sickness). Available online: [https://www.who.int/news-room/fact-sheets/detail/trypanosomiasis-human-african-\(sleeping-sickness\)](https://www.who.int/news-room/fact-sheets/detail/trypanosomiasis-human-african-(sleeping-sickness)) (accessed on 13 January 2023).
4. World Health Organization (WHO). Leishmaniasis. Available online: <https://www.who.int/news-room/fact-sheets/detail/leishmaniasis> (accessed on 13 January 2022).
5. Burza, S.; Croft, S.L.; Boelaert, M. Leishmaniasis. *Lancet* **2018**, *392*, 951–970. [CrossRef] [PubMed]
6. Simarro, P.P.; Cecchi, G.; Franco, J.R.; Paone, M.; Diarra, A.; Ruiz-Postigo, J.A.; Fèvre, E.M.; Mattioli, R.C.; Jannin, J.G. Estimating and Mapping the Population at Risk of Sleeping Sickness. *PLoS Negl. Trop. Dis.* **2012**, *6*, e1859. [CrossRef] [PubMed]
7. World Health Organization (WHO). Research Priorities for Chagas Disease, Human African Trypanosomiasis and Leishmaniasis. Available online: <https://apps.who.int/iris/handle/10665/77472> (accessed on 13 January 2023).
8. Rao, S.P.S.; Barrett, M.P.; Dranoff, G.; Faraday, C.J.; Gimpelewicz, C.R.; Hailu, A.; Jones, C.L.; Kelly, J.M.; Lazdins-Helds, J.K.; Mäser, P.; et al. Drug Discovery for Kinetoplastid Diseases: Future Directions. *ACS Infect. Dis.* **2019**, *5*, 152–157. [CrossRef] [PubMed]
9. Fersing, C.; Basmacıyan, L.; Boudot, C.; Pedron, J.; Hutter, S.; Cohen, A.; Castera-Ducros, C.; Primas, N.; Laget, M.; Casanova, M.; et al. Nongenotoxic 3-Nitroimidazo[1,2-*a*]Pyridines Are NTR1 Substrates That Display Potent in Vitro Antileishmanial Activity. *ACS Med. Chem. Lett.* **2019**, *10*, 34–39. [CrossRef] [PubMed]
10. Böhm, H.-J.; Flohr, A.; Stahl, M. Scaffold Hopping. *Drug Discov. Today Technol.* **2004**, *1*, 217–224. [CrossRef] [PubMed]
11. Terme, T.; Maldonado, J.; Crozet, M.P.; Vanelle, P.; Galtier, C.; Gueiffier, A. Synthesis of 2-Substituted-3-Nitroimidazo[1,2-*b*]Pyridazines as Potential Biologically Active Agents. *J. Heterocycl. Chem.* **2002**, *39*, 173–177. [CrossRef]
12. Mosmann, T. Rapid Colorimetric Assay for Cellular Growth and Survival: Application to Proliferation and Cytotoxicity Assays. *J. Immunol. Methods* **1983**, *65*, 55–63. [CrossRef]
13. Răz, B.; Iten, M.; Grether-Bühler, Y.; Kaminsky, R.; Brun, R. The Alamar Blue® Assay to Determine Drug Sensitivity of African Trypanosomes (*T.b. rhodesiense* and *T.b. gambiense*) in Vitro. *Acta Trop.* **1997**, *68*, 139–147. [CrossRef] [PubMed]
14. Baltz, T.; Baltz, D.; Giroud, C.; Crockett, J. Cultivation in a Semi-Defined Medium of Animal Infective Forms of Trypanosoma Brucei, T. Equiperdum, T. Evansi, T. Rhodesiense and T. Gambiense. *EMBO J.* **1985**, *4*, 1273–1277. [CrossRef] [PubMed]

**Disclaimer/Publisher’s Note:** The statements, opinions and data contained in all publications are solely those of the individual author(s) and contributor(s) and not of MDPI and/or the editor(s). MDPI and/or the editor(s) disclaim responsibility for any injury to people or property resulting from any ideas, methods, instructions or products referred to in the content.